Global Biogeochemical Cycles

RESEARCH ARTICLE
10.1029/2025GB008971

Land Carbon Sink Distribution in Northern Eurasia Is Driven by Climate Change

I. Melnikova[1,2], T. Yokohata[1], D. Schepaschenko[3], S. Sitch[4], and S. Maksyutov[1]

[1]Earth System Division, National Institute for Environmental Studies (NIES), Tsukuba, Japan, [2]Institute of Life and Environmental Sciences, Tsukuba University, Tsukuba, Japan, [3]International Institute for Applied Systems Analysis, Laxenburg, Austria, [4]Faculty of Environment, Science and Economy, University of Exeter, Exeter, UK

Key Points:

- The estimate of the Northern Eurasian carbon sink using multiple approaches is 0.47 ± 0.20 GtC year^{-1} for 2001–2015
- A pronounced spatial gradient along the mean temperature shapes the distribution of the carbon sink and its sensitivity to CO_2 emissions
- Despite rapid warming in northern regions, sink enhancement contributes less to the Northern Eurasian carbon sink due to low initial uptake

Supporting Information:

Supporting Information may be found in the online version of this article.

Correspondence to:

I. Melnikova,
irina.melnikova.fn@u.tsukuba.ac.jp

Citation:

Melnikova, I., Yokohata, T., Schepaschenko, D., Sitch, S., & Maksyutov, S. (2026). Land carbon sink distribution in Northern Eurasia is driven by climate change. *Global Biogeochemical Cycles*, *40*, e2025GB008971. https://doi.org/10.1029/2025GB008971

Received 5 NOV 2025
Accepted 5 JUN 2026

Author Contributions:

Conceptualization: I. Melnikova, S. Maksyutov
Data curation: I. Melnikova, D. Schepaschenko, S. Sitch
Funding acquisition: I. Melnikova, T. Yokohata, D. Schepaschenko
Investigation: I. Melnikova, T. Yokohata, D. Schepaschenko, S. Maksyutov
Methodology: I. Melnikova, S. Maksyutov
Supervision: T. Yokohata, D. Schepaschenko, S. Maksyutov
Writing – review & editing: I. Melnikova, T. Yokohata, D. Schepaschenko, S. Sitch, S. Maksyutov

Abstract Boreal forests are a major contributor to the global land carbon sink under rising CO_2 concentrations and a changing climate. Carbon sink estimates for Northern Eurasia from forest inventories, flux mapping, and remote sensing have moved toward convergence over the past decade, although substantial differences remain. Several bottom-up and top-down estimates exceed Russia's national greenhouse gas inventory values. Here, we combine data from four independent sources—machine-learning-based FLUXCOM, atmospheric inversion models, the TRENDY ensemble of dynamic global vegetation models, and CMIP6 Earth System Models—to assess the spatial and temporal characteristics of the Northern Eurasian net carbon sink and discuss the differences. Our multi-approach assessment yields a regional estimate of 0.47 ± 0.20 GtC year^{-1} for the 2001–2015 period, which accounts for one-third of the global land carbon sink. CMIP6 model estimates are broadly consistent with those from other approaches, lending confidence to their future projections, although regional differences persist across individual models. We find a pronounced spatial flux gradient from south to north and west to east along a mean temperature gradient, with stronger carbon sinks in the warmer southern regions and weaker sinks in the cooler northeastern regions. Despite rapid warming in the northern parts of Northern Eurasia, CO_2- and warming-induced carbon sink enhancement contributes little to the overall regional sink due to its initially low net productivity. These results underscore the importance of forest productivity in shaping the terrestrial carbon sink and provide a multi-perspective view of its evolution under continued anthropogenic forcing.

Plain Language Summary Boreal forests, which cover much of Northern Eurasia, play an important role in absorbing carbon dioxide from the atmosphere, helping to slow climate change. Over the past decade, estimates of how much carbon these forests absorb have become more consistent, but they still differ. Some estimates are much higher than Russia's national inventory report. Here, we combined information from four independent sources, ranging from machine learning products to process-based models. We found that from 2001 to 2015, Northern Eurasia absorbed about 0.47 billion tonnes of carbon each year—around one-third of the total global land carbon sink. We also found strong patterns in how the carbon sink changes across the region. It decreases from warmer southern areas toward colder northern areas and from west to east across the region. Despite rapid warming in the north, the increase in carbon absorption is small because these areas started with very low carbon storage and also compensate for rising emissions from thawing permafrost. This means that forest characteristics, such as forest structure, play an important role in how much carbon can be absorbed.

1. Introduction

Boreal forests play a vital role in the global carbon cycle, acting as a significant sink of atmospheric CO_2. The boreal biome in Northern Eurasia, largely within Russia, forms one of the largest continuous forest regions on Earth, accounting for approximately 20% of global forest cover (Krankina et al., 2004; Schepaschenko et al., 2015). It is widely recognized as a key contributor to the global land carbon sink, and its future trajectory under climate change carries major implications for global carbon budget assessments and climate feedback (Ciais et al., 2020; McDowell et al., 2020; Sitch et al., 2024). Boreal forest is also a major climate tipping element (McKay et al., 2023).

Despite its global importance, the magnitude and variability of the land carbon sink in Northern Eurasia remain uncertain, with a large variation in the estimates (Ciais et al., 2020; Deng et al., 2022; Dolman et al., 2012; Romanov et al., 2022; Schepaschenko et al., 2021; Sitch et al., 2024). Recent advances in forest inventories,

remote sensing, and atmospheric inversions have brought bottom-up and top-down estimates closer together, with many converging around a net land sink of ca. 0.3–0.4 GtC year^{-1} (Deng et al., 2022; Romanov et al., 2022; Schepaschenko et al., 2021; Sitch et al., 2024). These approaches come closer to the estimates reported in Russia's national greenhouse gas inventory (Romanov et al., 2022; Romanovskaya et al., 2020, 2022), which has recently been reassessed at ca. 0.3 GtC year^{-1} based on the results of the recent forest inventory by Romanovskaya et al. (2025) (Table S1 in Supporting Information S1). Still, the discrepancies limit confidence in regional greenhouse gas reporting and hinder our ability to assess the impact of forest management and climate mitigation strategies on the carbon cycle. More recently, A. Shvidenko et al. (2025) synthesized bottom-up and top-down approaches with a central estimate of 0.6 GtC year^{-1}. Process-based models, including Dynamic Global Vegetation Models (DGVMs) and Earth System Models (ESMs), offer a complementary perspective. Unlike inventory or flux-based methods, models can simulate the carbon–climate–vegetation system self-consistently, accounting for feedback among CO_2 concentrations, temperature, precipitation, land use, and vegetation dynamics (Sitch et al., 2024). However, model estimates themselves vary widely and are rarely benchmarked against observational constraints in a consistent spatial framework.

The drivers of the Northern Eurasian carbon balance exhibit strong regional particularities that distinguish the biome from other major forest regions. The region experiences some of the most pronounced warming globally due to Arctic amplification, yet vast areas remain under persistently cold climatic conditions that constrain vegetation growth (Terrer et al., 2019). Widespread nutrient limitations, particularly nitrogen scarcity, further limit the forest's capacity to sequester carbon even under elevated atmospheric CO_2. Carbon losses from wildfires and land-use change are substantial, with frequent extreme fire years causing large interannual variability in the carbon budget (Fan et al., 2023; Isaev et al., 2002; Kukavskaya et al., 2013; Ponomarev et al., 2023). Wildfires are a dominant disturbance in the region, particularly east of the Ural Mountains, where large fires account for a substantial share of the burned area in central Siberia (Fan et al., 2023; Krankina et al., 2004; Kukavskaya et al., 2013; A. Z. Shvidenko & Schepaschenko, 2013). Extreme fire years have occurred frequently over the past two decades, including 2003, 2006, 2008–2009, 2010, 2012, 2014, and 2019–2021 (Kharuk et al., 2021; Zheng et al., 2021). Socioeconomic transitions have also left a lasting imprint: during Russia's shift to a market economy in the early 1990s, timber harvests declined sharply, active reforestation decreased, and widespread agricultural abandonment followed. Much of this abandoned land has since transitioned to young deciduous forests, altering both carbon storage and flux dynamics (Krankina et al., 2004; Wendland et al., 2014). Finally, sparse observational networks across this vast and remote area limit the ability to validate models and monitor ongoing changes in carbon stocks and fluxes. In recent years, Russia has actively expanded its carbon observation network (such as RITM CARBON, https://ritm-c.ru/en/main/) and launched the second cycle of the national forest inventory (Filipchuk et al., 2023; https://roslesinforg.ru/services/gil/). However, access to these data remains limited.

In this study, we synthesize evidence from several independent sources to evaluate the spatial characteristics of the land carbon sink in Northern Eurasia within the borders of Russia, as defined by REgional Carbon Cycle Assessment and Processes (RECCAP) project (Ciais et al., 2020). The data sources include a machine learning–based product of net ecosystem exchange, trained on eddy covariance flux tower, climate and satellite data FLUXCOM (Jung et al., 2020; Nelson et al., 2024), ensemble of atmospheric inversions (INV), which infer carbon fluxes from CO_2 observations and transport models, contributed to Global Carbon Budget 2024 (GCB2024; Luijkx et al., 2024), the TRENDY ensemble of process-based terrestrial biosphere models (Sitch et al., 2024) and Coupled Model Intercomparison Project Phase 6 (CMIP6) ESMs, which simulate past and future carbon cycle feedback under standardized forcing conditions (Eyring et al., 2016). By comparing both historical changes and driver-specific model experiments, we discuss the differences between approaches. We aim to further improve our understanding of the Northern Eurasian carbon sink's response to CO_2 increases and climate change, ultimately enhancing our estimates. Our findings help contextualize past estimates, benchmark model performance, and clarify the role of CO_2 fertilization versus climate variability in shaping the terrestrial carbon sink across this globally significant forested region.

2. Data and Methods

Here, we combined multiple independent data sets to assess the variability of the land carbon sink across Northern Eurasia (Table 1 and Table S2 in Supporting Information S1).

Table 1
Data Sets Used in This Study for the Analysis of Carbon Fluxes

Data set	Spatial resolution	Period	Reference
Machine-learning-based			
FLUXCOM RS	0.0833°	2001–2015	Jung et al. (2020)
FLUXCOM-X	0.05	2001–2021	Nelson et al. (2024)
Machine-learning-based algorithm, constrained with inversions			
INV-FLUXCOM	0.5°	2001–2017	Upton et al. (2024)
Top-down (inversions)			
GCB2024 inversions	1°	1976–2023	Luijkx et al. (2024)
Bottom-up (DGVMs, ESMs)			
TRENDY	0.5°	1700–2022	Sitch et al. (2024)
CMIP6	Model-dependent	1850–2014 historical + 2015–2022 SSP5-8.5 simulation outputs	Eyring et al. (2016)

FLUXCOM is a machine-learning-based–based estimate of net ecosystem exchange (NEE) that integrates eddy covariance flux tower observations with remote sensing (Jung et al., 2020; Nelson et al., 2024). Here we use monthly gridded FLUXCOM produced in the remote sensing setup (FLUXCOM RS) in which fluxes are estimated from Moderate Resolution Imaging Spectroradiometer (MODIS) satellite data at 0.0833° spatial resolution covering the period 2001–2015 (Jung et al., 2020). In addition, we used a newer FLUXCOM product, FLUXCOM-X-BASE, at 0.05° spatial resolution covering the period 2001–2021 (Nelson et al., 2024).

We also use a machine-learning-based product, FLUXCOM, constrained with inversions (INV-FLUXCOM) by Upton et al. (2024). This product is based on the FLUXCOM utilizing meteorological and remotely sensed drivers (RS + METEO) with an ERA5 forcing ensemble (Jung et al., 2020; Tramontana et al., 2016). They are then constrained, using five models from the ensemble of atmospheric inversions of GCB2022 based on surface observations (Upton et al., 2024). The INV-FLUXCOM provides NEE at 0.5° spatial resolution for the 2001–2017 period.

For the top-down approach, we use fossil cement adjusted land flux of an ensemble of 14 gridded atmospheric inversion models prepared for the Global Carbon Budget 2024 (GCB2024), available at 1° spatial resolution covering the period 1976–2023 (Luijkx et al., 2024). The available period varies among models (Table S2 in Supporting Information S1).

For the bottom-up approach, we analyze results from the TRENDY version 12 ensemble of process-based terrestrial biosphere models (Sitch et al., 2024). TRENDY simulations account for historical changes in climate, atmospheric CO_2, and land use. We use monthly net biome productivity (NBP) outputs from the S3 protocol simulations of 17 TRENDY models, provided at 0.5° resolution for the period 1700–2022 (period and resolution vary between models, see Table S2 in Supporting Information S1). To isolate the effects of atmospheric CO_2 from those of climate change on the land carbon sink, we also analyze outputs from the S1 CO_2-only (time-invariant "pre-industrial" climate and land use mask) and S2 CO_2 and climate only (time-invariant "pre-industrial" land use mask) protocols.

Finally, we include outputs from CMIP6 historical simulations (Table S2 in Supporting Information S1). CMIP6 models simulate carbon fluxes within a self-consistent framework that incorporates hydrology, energy balance, and vegetation dynamics, enabling the assessment of past and projected land carbon sink dynamics and feedback. We use NBP outputs at each model's native resolution for the historical period (1850–2014) and for future projections (2015–2022) under the "fossil-fueled development" pathway (SSP5-8.5). To isolate the effects of atmospheric CO_2 from those of climate change on the land carbon sink, we also analyze outputs from the biogeochemically coupled historical and SSP5-8.5 simulations, in which only the biosphere responds to rising CO_2 levels, while the climate remains fixed. For the comparison of carbon fluxes, we use NBP values, assuming them to be opposite in sign to NEE.

In addition to carbon flux estimates, we use forest stock volume (m^3 ha^{-1}) estimates for Russian forests around 2014, derived from a combination of National Forest Inventory and remote sensing data (Schepaschenko

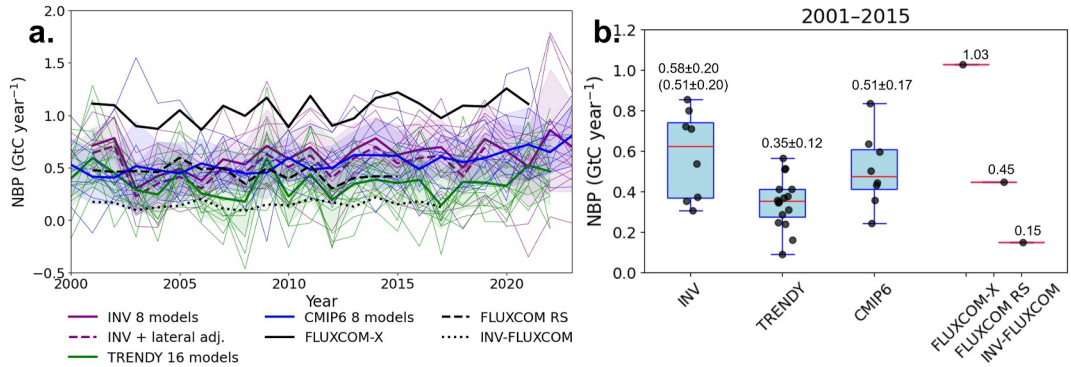

Figure 1. NBP (GtC year^{-1}) estimates of the Northern Eurasia region by all considered approaches. (a) Time series of NBP by each model in different approaches (thin lines) and the mean of each approach (thick lines). Inversion-based estimates are shown without correction for lateral riverine fluxes (solid purple line) and with lateral flux adjustment, according to Deng et al. (2022) (dashed purple line). The inter-model means are estimated only from the models that cover the 2001–2015 period. FLUXCOM-X, FLUXCOM RS and INV-FLUXCOM are considered separately as independent approaches. (b) Box plots of 2001–2015 NBP. Black dots show individual model estimates. Red lines indicate ensemble medians. The bottom and top edges of each box represent the first (25th percentile) and third (75th percentile) quartiles, respectively. Whiskers extend to the most extreme values within 1.5 times the interquartile range from the box edges. The numbers above each box indicate the 2001–2015 mean ±1 standard deviation.

et al., 2021). We also include estimates of forest age and average annual increment for Russian forests (Schepaschenko et al., 2018). Together, these data sets enable us to benchmark the multi-approach estimates and to analyze the spatial variation of the carbon sink across Northern Eurasia along gradients of forest characteristics. We estimate the average annual increment for Russian forests as a fraction of the stock volume by dividing the forest stock volume by age. We utilize landscape fire emissions from the 5th version of the Global Fire Emissions Database (GFED5) for the 2001–2022 period, available monthly at a resolution of 0.25°, to identify areas of fire disturbances. We use national land-use change (LUC) carbon dioxide emissions from GCB2024 (Friedlingstein et al., 2025; Gasser et al., 2020; Hansis et al., 2015; Houghton & Castanho, 2023; Qin et al., 2024). We use permafrost extent for the Northern Hemisphere (version 4 data) from the European Space Agency's (ESA) Climate Change Initiative (CCI) Permafrost project (Westermann et al., 2024b) and CRU TS4.09 mean temperature data (Harris et al., 2020) to analyze the spatial variation of the carbon sink along the climatic gradient.

3. Results and Discussion

3.1. Regional Carbon Sink Estimates

We find consensus among carbon sink estimates produced by different approaches for the 2001–2015 period (Figure 1). Northern Eurasia ecosystems are a carbon sink of 0.47 ± 0.20 GtC year^{-1} (mean ± standard deviation) or 0.51 ± 0.24 GtC year^{-1} (median ± interquartile range), as consistently estimated across five approaches (with two FLUXCOM products, FLUXCOM-X and FLUXCOM RS, grouped as one approach). Our multi-approach estimates are slightly lower than the recent other multi-approach estimates of 0.64 ± 0.17 GtC year^{-1} by A. Shvidenko et al. (2025) and 0.73 ± 0.22 GtC year^{-1} by Ciais et al. (2020) for the 2001–2009 period. Nevertheless, this sink accounts for one-third of the global net land carbon sink (when accounting for the land-use change emissions) for the same period, as estimated by the GCB2024 (Friedlingstein et al., 2025).

The largest divergence occurs within the FLUXCOM estimates, ranging from the lowest value in INV-FLUXCOM to the highest in FLUXCOM-X (Figure 1). Notably, FLUXCOM estimates do not explicitly account for the effects of CO_2 fertilization, land-use disturbances, or fire emissions—they are only indirectly captured through satellite-derived inputs (Jung et al., 2020). Land-use change and fire emissions reach up to 0.5 GtC year^{-1}, depending on the year (Figure S1 in Supporting Information S1). Consequently, as also noted by product authors, FLUXCOM-based estimates should be interpreted with caution, particularly when assessing interannual variability or temporal trends (Jung et al., 2020; Nelson et al., 2024). The latter three modeling approaches exhibit closer agreement, with inversions providing the highest mean estimate at 0.58 ± 0.20 GtC year^{-1} (at 0.51 ± 0.20 GtC year^{-1} when adjusted for riverine fluxes), followed by CMIP6

ESMs at 0.51 ± 0.17 GtC year^{-1} and TRENDY DGVMs at 0.35 ± 0.12 GtC year^{-1} for the 2001–2015 period. All approaches indicate a weakly positive but statistically non-significant temporal trend in the regional carbon sink over this period.

The inversion-based fluxes represent net surface–atmosphere CO_2 exchange integrated over the region and therefore do not explicitly account for lateral carbon transfers such as river export or trade of harvested biomass products. Estimates of these fluxes for Russia remain uncertain, ranging from about 0.08 GtC year^{-1} (Deng et al., 2022) to 0.14 GtC year^{-1} with an uncertainty of roughly 50% (Ciais et al., 2020). Although relatively small compared to the regional sink estimated here, these fluxes may influence comparisons between flux-based estimates and stock-based estimates, such as forest carbon sinks derived from inventory data. Process-based models also differ in their treatment of lateral fluxes, as some TRENDY DGVMs and CMIP6 ESMs implicitly account for harvest removal or river export, whereas others omit them. Our results should therefore be interpreted with this caveat in mind.

As a sensitivity test, we evaluated the mean land carbon sink for the 2015–2022 period using available modeling approaches (Figure S2 in Supporting Information S1). Although FLUXCOM data are not available for these years, many GCB2024 inversion models—particularly those incorporating satellite data—extend from 2015 onward. For CMIP6, we use outputs from the SSP2-4.5 scenario, given that the historical simulations end in 2014. The estimated Northern Eurasian net land carbon sink for 2015–2022 is 0.51 ± 0.11 GtC year^{-1} (mean ± standard deviation) or 0.55 ± 0.13 GtC year^{-1} (median ± interquartile range), closely aligning with our 2001–2015 estimate. Among the approaches, the GCB2024 inversions yield both the highest sink values and the widest inter-model spread. This large spread may reflect differences in the inverse system design and how atmospheric transport is represented across inversion systems. In particular, transport models that simulate a larger seasonal amplitude of atmospheric CO_2 at northern high-latitude stations, which can be attributed to weaker vertical mixing, happen to infer smaller regional carbon sinks. A qualitative indication of this relationship emerges from comparisons of transport model evaluations by Remaud et al. (2023) with inversion-based estimates of the Russian carbon sink (Deng et al., 2022). Models such as MIROC and NICAM/NISMON show relatively large simulated seasonal amplitudes for COS tracer, while also producing comparatively smaller Russian carbon sink estimates. However, because the set of transport model versions may differ between studies, this observation should be interpreted cautiously. Previous studies have shown that transport models differ in representing diabatic mixing across moist isentropes in the mid-latitudes, highlighting the need for further investigation (Jin et al., 2024, 2025; Remaud et al., 2023).

TRENDY DGVMs estimate a Northern Eurasian carbon sink nearly half the size of that from GCB2024 inversions (Figure 1b). This issue has been explored before and attributed to overestimating the fire emissions and underestimating forest regrowth by TRENDY models due to the lack of forest demography representation (O'Sullivan et al., 2024). In fact, forest age, demography and wood harvest are absent in most TRENDY DGVMs (Sitch et al., 2024).

The large spread among CMIP6 ESMs—greater than that of TRENDY despite fewer models—may be partly due to differences in simulated surface climate. While TRENDY DGVMs use prescribed climate variables, CMIP6 models represent fully coupled atmosphere–land–ocean interactions. Notably, several of the included ESMs are known as "hot" models, which have been shown to overestimate historical surface air temperature trends (Tokarska et al., 2020). However, additional analysis suggests that the inter-model differences in CMIP6 regional carbon sink estimates are driven primarily by carbon cycle processes and carbon–climate feedbacks, rather than by differences in simulated warming levels (Figure S3 in Supporting Information S1). We found a weak, insignificant negative correlation between CMIP6-simulated past warming trends and the 2001–2015 carbon sink in Northern Eurasia.

3.2. Spatial Variation of Carbon Sink

The spatial variation of the land carbon sink across Northern Eurasia reveals a consistent multi-approach signal: a regional maximum in the western mid-latitudes around 55–60°N, followed by a decline both northward and eastward, despite more warming in the northern high latitudes (Figure 2 and Figures S4–S6 in Supporting Information S1). All approaches indicate stronger carbon sinks in the forested areas of European Russia and the southern parts of West Siberia. However, notable differences remain in the spatial patterns and magnitudes of the land carbon sink across models. Despite the limitations of FLUXCOM products (outlined in the previous section),

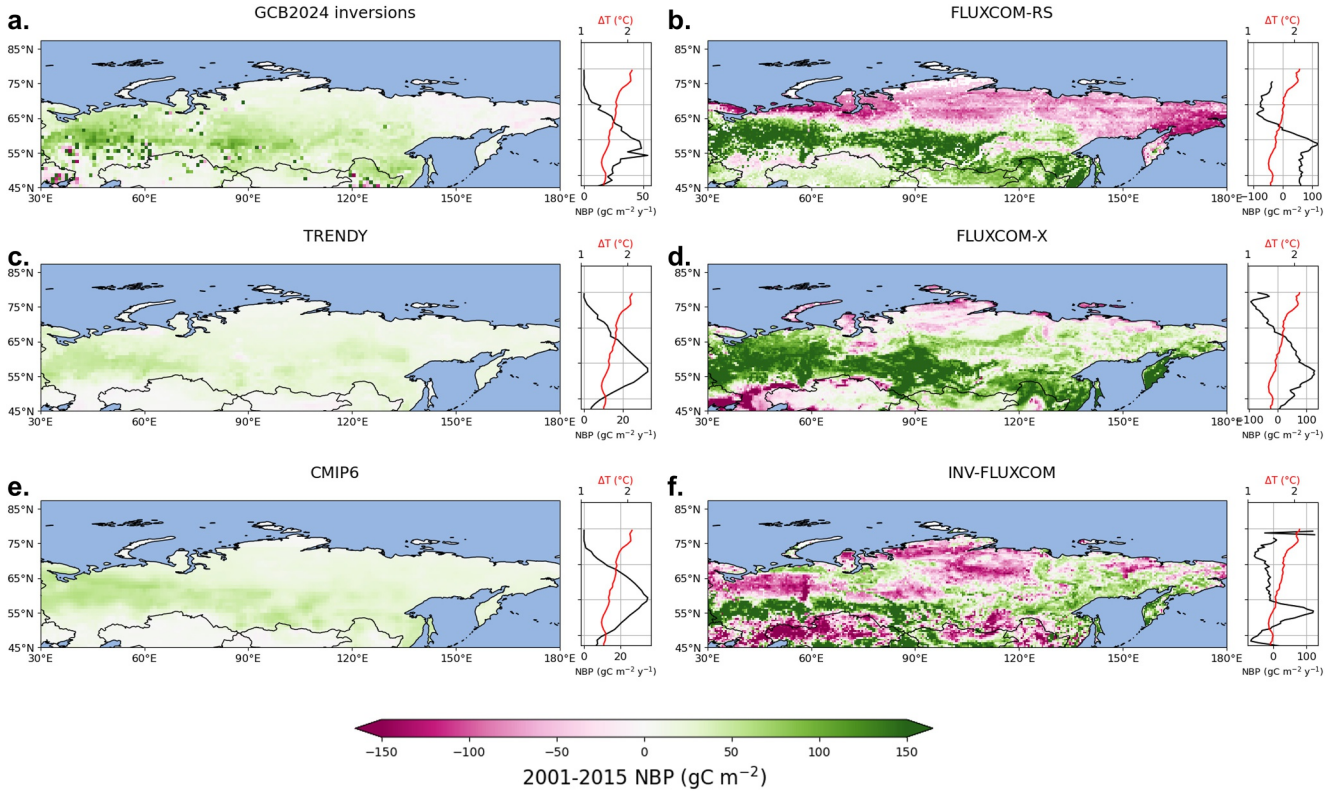

Figure 2. Spatial variation of the mean 2001–2015 NBP (gC m^{-2} $year^{-1}$) estimates of the Northern Eurasia region by all considered approaches. (a) Mean of 8 atmospheric inversions of GCB2024, (b) FLUXCOM-RS, (c) mean of 16 TRENDY DGVMs, (d) FLUXCOM-X, (e) mean of 8 CMIP6 ESMs, and (f) INV-FLUXCOM. The latitudinal mean NBP (gC m^{-2} $year^{-1}$) in black and CRU land surface air temperature (°C) in red are shown on the right side of each panel.

their use of eddy-covariance and satellite data is a key advantage. Nevertheless, none of the three modeling approaches, GCB2024 inversions, TRENDY and CMIP6, reproduce the carbon source areas identified by FLUXCOM.

Among all products, the FLUXCOM product constrained by atmospheric inversions exhibits the greatest divergence in the spatial distribution of the carbon sink, with many areas, including parts of European Northern Eurasia, functioning as carbon sources. The INV-FLUXCOM authors also reported a lower performance of their product for boreal regions, including Russia (Upton et al., 2024). These discrepancies may arise from several factors. FLUXCOM products rely on flux tower observations for training, and the sparse distribution of eddy covariance sites in boreal ecosystems may limit their ability to represent carbon flux variability in Northern Eurasia. Inversion-based constraints also depend strongly on the representation of atmospheric transport, which can introduce additional uncertainty in regional flux attribution. Process-based models may further differ in their representation of key ecosystem processes, such as forest demography and disturbance dynamics. In addition, the inversion ensemble used to constrain the INV-FLUXCOM product differs from the inversion models analyzed in this study, and updates to inversion systems can produce substantial differences between model versions. Nevertheless, hybrid approaches that combine flux-tower–based products with atmospheric inversion constraints, such as INV-FLUXCOM, offer promising potential for improving regional carbon flux estimates by integrating ecosystem observations with atmospheric signals. However, because the INV-FLUXCOM data set used here is only available for 2001–2017, we could not evaluate this potential for the recent (2019–2021) extreme disturbance years.

The spatial patterns of the land carbon sink from inversion models (Figure S4 in Supporting Information S1, shown for 2001–2015 and 2015–2023 periods) display a broadly consistent west-to-east and south-to-north gradient, with most models identifying stronger uptake in the forested regions of European Russia and parts of West Siberia. However, the magnitude and spatial distribution of these sinks vary substantially across models. Some models, such as CAMS, CT-NOAA and CTE2024, show strong carbon uptake over broad areas of central

and eastern Russia, while others (e.g., CAMS-Satellite, Jena CarboScope and NFTVAR) indicate large areas of carbon source in the northeastern Northern Eurasia, broadly consistent with the FLUXCOM products. Many inversions, such as CAMS, CTE2024, NISMON-CO2, GCASv2, GONGGA and NFTVAR, also display localized sources in eastern Russia, consistent with fire emission hotspots (Figure S7a in Supporting Information S1). Differences in input data (surface vs. satellite), transport model configurations, and data assimilation methods contribute to the observed spread in spatial patterns.

TRENDY DGVMs show a smoother spatial pattern with weaker carbon sinks overall, consistent with their lower regional mean NBP. Most models simulate strong uptake in European Russia (Figure S5 in Supporting Information S1). However, there is notable variability in both the magnitude and extent of the sink. Models such as OCN, YIBs and ELM simulate widespread uptake, even in the eastern high latitudes, while others show more fragmented or localized sinks, sometimes accompanied by adjacent source regions. Our analysis did not confirm that variations in ecosystem process representation (e.g., nitrogen cycle), disturbance regimes (e.g., fires), or forest demography among DGVMs explain the differences in the spatial patterns of land–atmosphere carbon exchange (Table S2 and Figure S5 in Supporting Information S1).

CMIP6 ESMs broadly capture the latitudinal gradient of the land carbon sink in Northern Eurasia, with stronger uptake concentrated in the taiga zone between ~50°N and 65°N (Figures 1 and 2 and Figure S6 in Supporting Information S1). Most models simulate a widespread carbon sink in European Russia and western Siberia. However, like in other multi-model approaches, both the spatial patterns and magnitudes of the sink vary considerably across models. CNRM-ESM2-1, MRI-ESM2-0 and IPSL-CM6A-LR simulate widespread sinks in all Northern Eurasia, while others, such as ACCESS-ESM1-5, CanESM5 and NorESM2-LM, show a more pronounced climatic gradient in NBP. These inter-model differences likely stem from variations in land surface schemes and carbon cycle parameterizations, as discussed in the section above.

In contrast, the FLUXCOM-X and FLUXCOM RS products show strong spatial contrasts, with pronounced carbon sink areas in southwestern Northern Eurasia and extensive carbon source regions, particularly in the north. These differences in spatial structure reflect underlying methodological contrasts: while inversions and ESMs are driven by process-based simulations and atmospheric constraints, FLUXCOM products rely on eddy-covariance data and satellite-observed vegetation activity. Notably, there are also differences between the FLUXCOM RS and the newer FLUXCOM-X product. The latter displays a decrease in carbon sink toward the northeast of Northern Eurasia but locates carbon source areas only at high northern latitudes.

Figure 3 illustrates the relationship between the land carbon sink and forest productivity across Northern Eurasia, as captured using various approaches. In this analysis, we benchmark land sink estimate approaches against the annual average forest increment (Schepaschenko et al., 2018), calculated as the growing stock volume divided by forest age, as a proxy for the potential of forests to accumulate biomass over time (Figure 3a). This metric integrates both forest structure (biomass) and developmental stage (age), offering a more dynamic measure of productivity than growing stock volume alone. We approximate productivity as an annual increment derived from the ratio of stand volume to stand age. Although this metric implicitly assumes approximately linear growth and therefore does not capture nonlinear stand development in mature or disturbed stands, it provides a first-order proxy for site productivity, that is, consistently available across the regional forest inventory data. Annual increment reflects the capacity of forests to act as carbon sinks, as higher increment values indicate younger, actively growing stands or productive ecosystems.

The FLUXCOM RS and TRENDY approaches showed the strongest correlations between NBP and forest annual increment estimates ($R = 0.57$ and $R = 0.46$, $p < 0.05$). The weaker west-to-east climatic gradient in the FLUXCOM-X land carbon sink (Figure 2d) leads to a lower correlation with forest productivity (Figure 3d). The lowest correspondence is observed for the GCB2024 inversion ensemble and INV-FLUXCOM (Figures 3b and 3e). To investigate the causes of this poor agreement, we examined scatterplots for individual inversion models (Figure S8 in Supporting Information S1). While some inversions show reasonable correspondence with forest annual increment (e.g., CAMS, Jena CarboScope, NISMON-CO2, NFTVAR, GCASv2), many others exhibit substantial discrepancies, indicating the need for further improvement. Examination of the prior fluxes suggests that models showing stronger correlations in the posterior estimates often also exhibit similar relationships in the prior NBP fields, indicating that part of the signal may originate from the priors used in the inversion systems (not shown). A more thorough investigation would be required to disentangle the relative influence of prior fluxes and

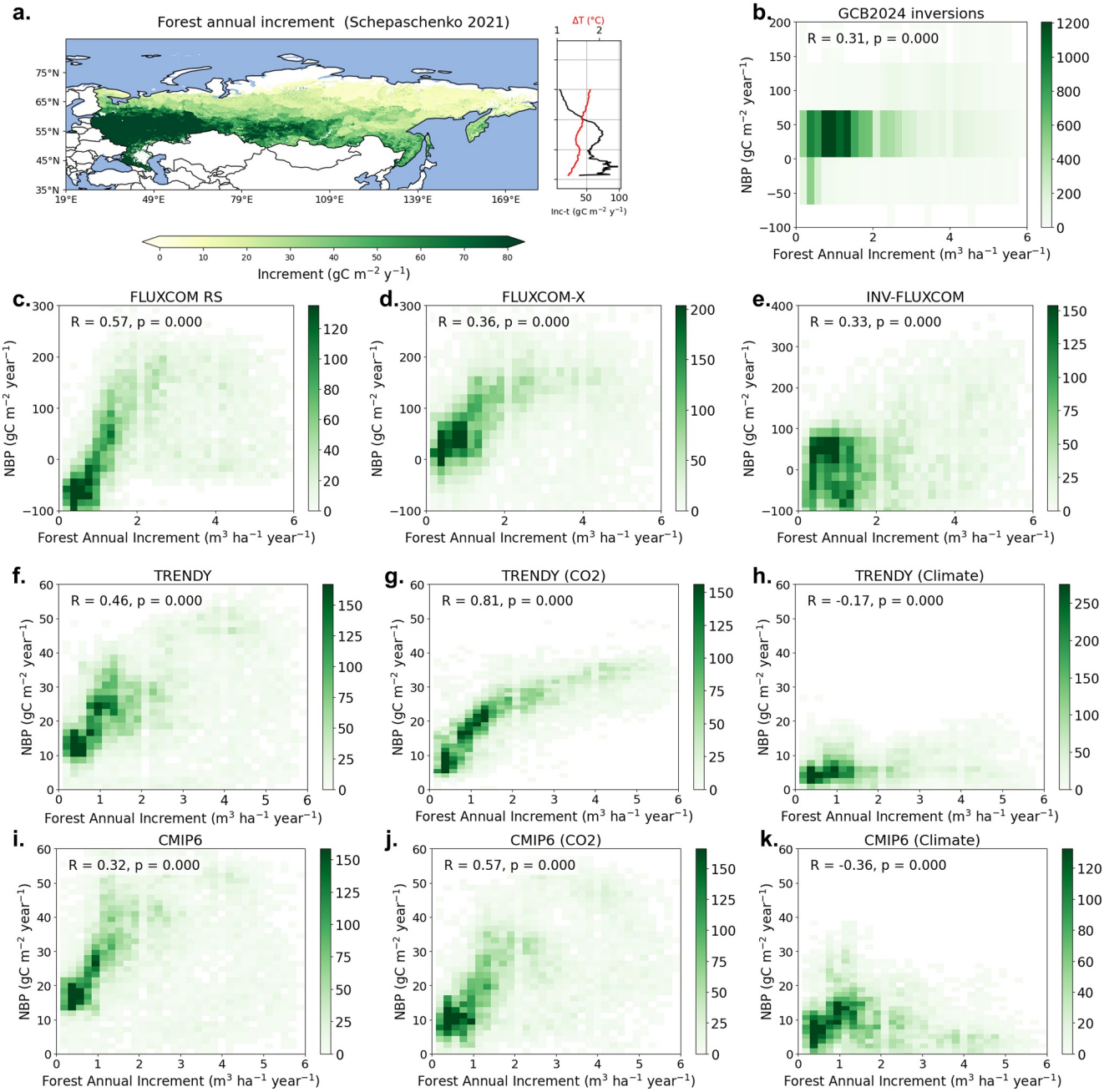

Figure 3. (a) Spatial variation of forest annual increment (gC m^{-2} $year^{-1}$). (b–k) Scatter density plots of NBP (gC m^2 $year^{-1}$) versus forest annual increment (m^3 ha^{-1} $year^{-1}$) for Northern Eurasia, averaged over the 2001–2015 period. (b) GCB2024 inversions, (c) FLUXCOM RS, (d) FLUXCOM-X, (e) INV-FLUXCOM, (f) TRENDY, (g) TRENDY CO2-only simulation, (h) TRENDY climate-only simulation, (i) CMIP6, (j) CMIP6 CO2-only simulation and (k) CMIP6 climate-only simulation. Color shading indicates the sum of grid-cell areas (in thousand km^2) within each bin. Correlation coefficients (*R*) and *p*-values are shown in each panel.

observational constraints. In line with this finding, the inversion-constrained INV-FLUXCOM product also performs worse than FLUXCOM products.

The TRENDY and CMIP6 models show reasonable agreement with forest annual increment, which is dominated by CO_2 fertilization effects on the land carbon sink, as discussed in detail in the following section. Although we cannot identify a single best or most accurate data set for estimating the Northern Eurasian carbon sink, we summarize here the advantages and limitations of each approach, with the aim of providing recommendations to improve future estimates (Table 2). All the approaches considered in this study yield higher estimates of the

Table 2
Advantages and Limitations of Approaches Used in This Study for Estimating the Northern Eurasian Carbon Sink

Data set	Advantages	Disadvantages
FLUXCOM RS	Use of stationary eddy-covariance flux estimates and satellite observations	Few eddy-covariance sites in Northern Eurasia, absence of site estimates during the cold season, no explicit accounting for effects of CO_2 fertilization, land-use disturbances, or fire emissions
FLUXCOM-X	Same as FLUXCOM RS but more sites available	Same as FLUXCOM RS
INV-FLUXCOM	A "dual-constraint" (combination of top-down and bottom-up approaches)	Confirmed product's lower performance in the boreal region, inconsistent spatial patterns with other approaches (emerging approach)
GCB2024 inversions	Direct use of atmospheric CO_2 measurements and fire emissions	Issues with atmospheric transport representation across inversion systems, lower quality during the boreal winter; depend on prior estimates to varying degrees, largely controlled by the number of atmospheric observations and their sensitivity to NBP
TRENDY	Process-based approach, large model ensemble, possibility for attribution of land sink to the changes in CO_2, land-use and climate	Absence of representation of some important ecosystem processes for the region in some models (N cycle, fires, forest demography), underestimation of forest regrowth and overestimation of fire emissions, too large CO_2 effect on the land sink in permafrost areas
CMIP6	Process-based approach, simulation of land hydrology, energy balance and vegetation dynamics in a self-consistent framework, possibility for attribution of land sink to the changes in CO_2 and climate, future projections	Same as TRENDY, and lesser consistency of forcing data with observed climate, often lower resolution

carbon sink compared to the official national reports of the Russian Federation by Romanovskaya et al. (2022, 2025) (Figure S9 and Table S1 in Supporting Information S1). Previously, Romanov et al. (2022) suggested that the lower values reported in the country's official estimates result from: (a) assuming net-zero carbon uptake in mature forests, (b) excluding the carbon sink of unmanaged forests covering up to 21.6% of Russia's forest area, (c) reliance on outdated forest inventory data and (d) applying shallow soil depth limits when estimating soil carbon stocks. Although with a larger regional extent (RECCAP "Russia" region), our estimate of the net carbon sink is approximately three times higher than that of the official 2024 national report. However, in the 2025 report, the carbon sink was retrospectively reassessed and effectively doubled. The advantages of the carbon sink estimation approaches, outlined in Table 2, are consistent with the proposed explanations from previous studies and suggest concrete ways to improve national estimates. Strengthening the accuracy of these estimates is critical for designing effective climate-mitigation policies, enhancing the credibility of national greenhouse gas inventories, and supporting mechanisms such as carbon credits and international climate reporting.

3.3. Drivers of the Northern Eurasian Carbon Sink

The carbon sink decline northward and eastward, discussed in the previous sections, coincides with decreases in the mean surface air temperature and long-term surface air temperature increase (Figure S10 in Supporting Information S1), which in turn coincides with higher permafrost extent (Figure S7b in Supporting Information S1). Although the northeastern parts of Northern Eurasia are warming much faster than other regions and the global average, they still experience harsh climatic conditions, with mean annual temperatures remaining below zero and permafrost remaining largely intact. The persistence of cold conditions suggests that warming has not yet led to a widespread increase in the carbon sink capacity. Consequently, the NBP estimates reveal clear gradients with respect to mean temperature, temperature change, and latitude (Figures 4a–4c). Across all approaches, the carbon sink consistently peaks and then declines along both temperature and latitudinal gradients (Table S3 in Supporting Information S1). The maximum carbon sink occurs in areas with mean surface air temperatures above 0°C and warming levels of 1.2°C–1.5°C. Despite stronger warming in the northeast, the warming-induced enhancement of the net land carbon sink contributes little to the overall sink increase in Northern Eurasia. This is partly because much of the northern warming occurs in winter, when soils remain frozen and carbon sequestration is limited. We suggest that these carbon sink gradients are influenced by "site quality," often referred to as "bonitet" classes in Russian and Northern European forestry. Bonitet is a classification of site productivity that reflects how favorable

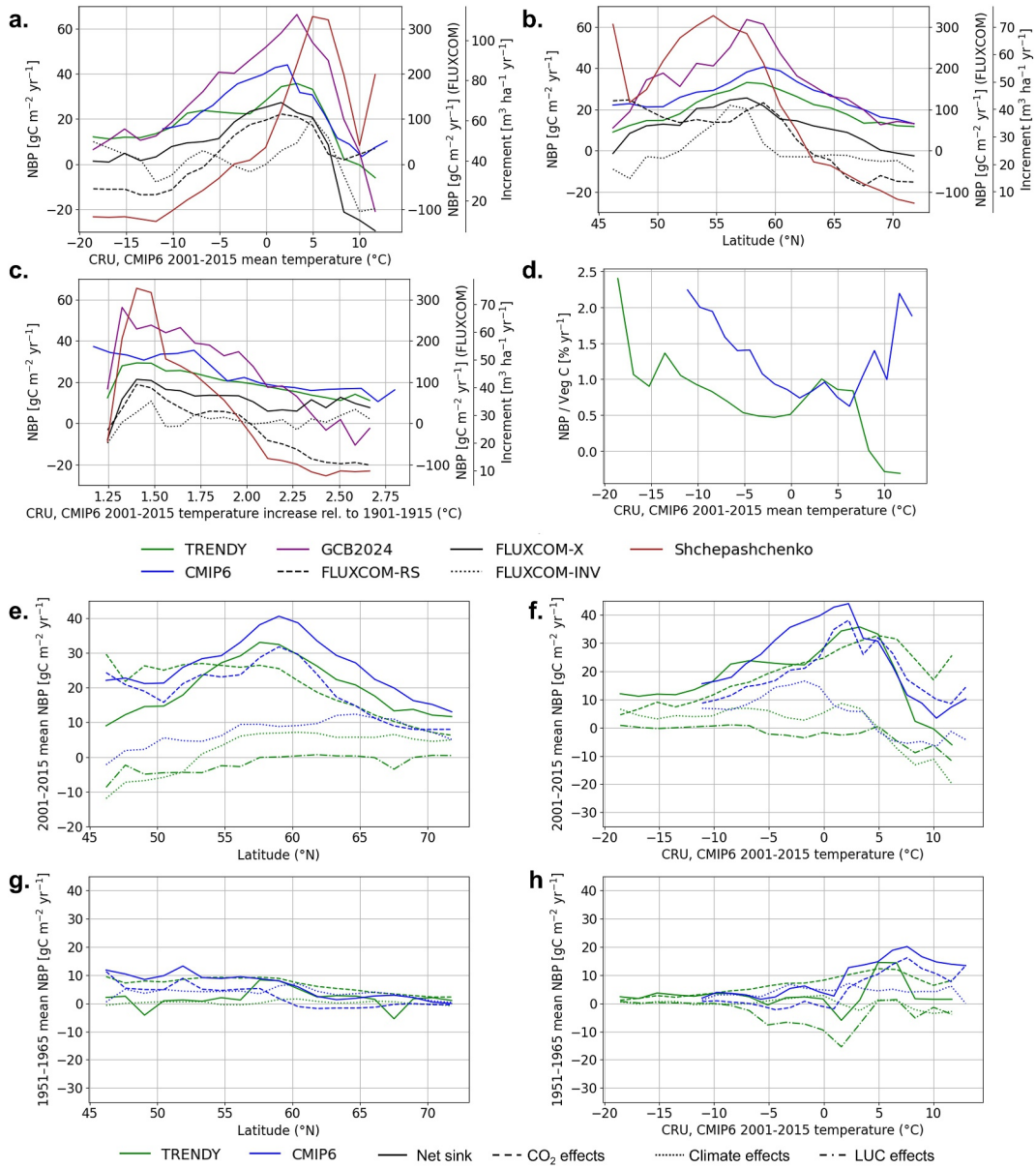

Figure 4. 2001–2015 mean NBP (gC m^{-2} year^{-1}) and forest annual increment (m^3 ha^{-1} year^{-1}) with respect to (a) CRU TS/CMIP6 2001–2015 mean surface air temperature (°C), (b) latitude (°N) and (c) mean surface air temperature change relative to 1901–1915 (°C) by considered approaches. Note that TRENDY, GCB2024 inversions, and CMIP6 NBP values are on the left *y*-axis, and 3 FLUXCOM products are on the right *y*-axis in the panels. The forest annual increment estimated by Schepaschenko et al. (2021) is given for reference. Panel (d) shows NBP relative to vegetation carbon pool (NBP/Veg C, % year^{-1}) versus mean surface air temperature change. Panels (e–h) show (e, f) 2001–2015 mean and (g, h) 1951–1965 NBP with respect to (e, g) latitude (°N) and (f, h) CRU TS/CMIP6 2001–2015 mean surface air temperature (°C) by TRENDY and CMIP6 ensemble means in the standard setups (solid lines) and experiments with isolated effects of CO_2 fertilization (dashed lines), climate (dotted lines) and land-use change (dash-dot lines).

a forest site is for tree growth, integrating measures such as tree height, volume, and biomass, and sometimes soil and habitat conditions (Romanovskaya et al., 2022). Although the forest area is larger in the eastern part of Northern Eurasia, the forests there have lower stock volumes, are generally older, with higher fire disturbance, and are less productive, corresponding to lower "bonitet" classes (Figure S11 in Supporting Information S1). Increases in net primary production due to warming and CO_2 fertilization are largely offset by higher heterotrophic respiration and emissions from thawing permafrost. Note that despite the smaller magnitude of carbon

sink enhancement, the effectiveness of the carbon sink, defined here as the ratio of NBP to aboveground biomass, increases in the colder areas of Northern Eurasia (Figure 4d).

The latitude of maximum NBP varies across approaches, from 48°N in FLUXCOM RS to 59°N in CMIP6, reflecting substantial differences in ecosystems. In the boreal zone, approximately 50°–56/58°N corresponds to the southern taiga, dominated by mixed forests, while ∼56/58°–62/64°N corresponds to the middle taiga, dominated by coniferous forests. Despite broad agreement on the peak and subsequent decline of the carbon sink along the warming gradient (Figures 4a and 4c), the TRENDY, CMIP6, and FLUXCOM-X products show a much smaller gradient in magnitude, and TRENDY and CMIP6 estimate a larger carbon sink in regions with mean temperatures below 0°C. As discussed in previous sections, these differences in sink magnitude require further investigation to reduce uncertainties.

Despite these differences, TRENDY and CMIP6 reproduce the temperature and latitudinal gradients of the carbon sink well enough to support attribution to CO_2 and climate drivers. Factorial simulations in both ensembles isolate these effects: CO_2-only experiments align closely with forest annual increment estimates (Figures 3f–3i), indicating a strong CO_2-fertilization effect in regions with high forest stock volume and high annual increments. In contrast, the climate-only runs contribute mainly to year-to-year variability in the land sink (Figures 3g–3j).

Latitudinal and temperature gradients of the land carbon sink by TRENDY and CMIP6 also indicate the dominant role of the CO_2 fertilization effect on the Northern Eurasian carbon sink (Figures 4e and 4f). In the CO_2-only experiments, the peak either coincides with (CMIP6) or lies south of (TRENDY) the peak of the net carbon sink. In the climate-only experiments, the latitudinal maximum of the carbon sink shifted poleward to ∼65°N. North of this maximum, TRENDY and CMIP6 indicate CO_2-driven increases and climate-driven changes of comparable magnitude, implying similar contributions of CO_2 and climate change. This attribution in the cold (sub-zero) regions by TRENDY and CMIP6 does not fully align with remote-sensing–based estimates (e.g., FLUXCOM). The strength of CO_2 fertilization in boreal ecosystems remains uncertain: free-air CO_2 enrichment (FACE) experiments in temperate–boreal forests are scarce and report mixed outcomes—ranging from increased biomass production to no detectable effect—particularly in late-successional, mature stands (Liu et al., 2024; Norby et al., 2024; Walker et al., 2019). Mature forests, which are abundant in eastern Northern Eurasia (Figure S11c in Supporting Information S1), are strongly constrained by harsh climate and nutrients, especially nitrogen, thereby limiting the CO_2 fertilization response (Liu et al., 2024; Norby et al., 2024). Taken together, these lines of evidence suggest that many process-based models (TRENDY, CMIP6) may overestimate CO_2 fertilization or underestimate carbon emissions due to permafrost thaw (Schuur et al., 2022) in cold boreal and permafrost-covered regions, helping to explain the weaker decline of the land carbon sink with latitude and temperature in these ensembles relative to other approaches. This issue requires rigorous investigation through targeted field observations and expanded boreal FACE experiments.

The Northern Eurasian land carbon sink has largely emerged as a consequence of anthropogenic activities over recent decades, as evident from comparisons of the latitudinal and temperature gradients of the land carbon sink between 1951–1965 and 2001–2015 (Figures 4e–4h). During the early period, the ecosystems of Northern Eurasia were nearly carbon neutral overall, with only the relatively warm western regions showing a weak sink driven by rising atmospheric CO_2 and early stages of climate warming. In contrast, by the early 21st century, a pronounced carbon uptake has developed across much of the region, accompanied by a distinct spatial shift in its peak intensity. The center of the land sink has moved eastward and northward, corresponding to areas that have experienced moderate warming (0°C–5°C relative to the 1901–1915 mean). Together, these trends indicate that the current Northern Eurasian sink is a relatively recent and human-modified feature of the global carbon cycle, shaped by the combined effects of climate forcing, ecological recovery, and socioeconomic drivers.

3.4. Future Perspectives

This study shows that CMIP6 models are broadly consistent with other approaches despite persistent regional differences (Figures 1 and 2). They also reproduce the attribution of land carbon sink changes to CO_2 and climate drivers in agreement with TRENDY DGVMs (Figures 4e–4h). These consistencies increase confidence in the representation of present-day carbon sink processes in CMIP6 models. However, agreement with present-day estimates does not necessarily imply reliable projections of future carbon sink dynamics, which depend on nonlinear processes such as disturbances, hydrological changes, nutrient limitation, permafrost carbon and

vegetation responses that remain uncertain and are incompletely represented in many CMIP6 models (Gier et al., 2024; Huang et al., 2022). Further work is therefore needed to assess how these processes may influence future carbon sink dynamics in Northern Eurasia.

Here, we focused primarily on the latitudinal and temperature gradients of the land carbon sink. However, recent studies highlight the increasing importance of droughts in shaping boreal carbon dynamics, particularly across Siberia (Fan et al., 2023; Li et al., 2025). The areas exhibiting the strongest carbon uptake—mainly in the central European part of Russia—are also regions without precipitation deficits (Figure S12 in Supporting Information S1), whereas drying trends are evident in the southern part of European Russia. The observed northward shift of the carbon sink peak—from 1951–1965 to 2001–2015—likely reflects this dependence of carbon uptake on moisture availability.

In contrast, the relatively drier conditions of eastern Siberia may limit the increase of its forest carbon sink with warming, a pattern likely reinforced by drought- and fire-induced disturbances (Fan et al., 2023; Li et al., 2025). At the same time, surface warming promotes permafrost thaw, which can locally enhance soil wetness and lead to waterlogging across extensive flat lowlands. Ecosystem responses in these regions—dominated by larch forests that are highly sensitive to soil moisture (Miyahara et al., 2011)—remain uncertain and warrant further detailed investigation.

Beyond Northern Eurasia, our approach—integrating multiple lines of evidence from models, data-driven products, and observations—can be applied to other regions globally. Such cross-data set comparisons enable a more comprehensive assessment of both past and future changes in land carbon sinks, while also revealing the strengths and limitations of each approach. However, recent disturbances such as large wildfire events may alter regional carbon flux patterns and may not be fully captured by some data-driven products, highlighting the importance of combining complementary approaches when assessing recent changes. Extending this framework beyond Northern Eurasia could improve our understanding of regional carbon–climate feedback and enhance the robustness of global carbon budget assessments.

4. Conclusions

Our multi-approach assessment synthesizes FLUXCOM, atmospheric inversions, TRENDY DGVMs, and CMIP6 ESMs to provide a comprehensive view of the Northern Eurasian land carbon sink. For 2001–2015, the ensemble mean is 0.47 ± 0.20 GtC year^{-1}—lower than some recent estimates yet accounting for roughly one-third of the global land sink. In the absence of a definitive ground truth, we do not rank the approaches. Instead, we evaluate their respective strengths and limitations and highlight priorities for reducing uncertainty. The broad consistency between CMIP6 ESMs and other data-driven estimates supports the credibility of their projections, although persistent regional mismatches underscore the need for improved process-based model representation of boreal ecosystems.

A pronounced spatial pattern along the temperature gradient shapes both the distribution of the sink and its sensitivity to anthropogenic forcing. The strongest sinks occur in the southern and western parts of Northern Eurasia, where a milder climate and larger forest stock volumes prevail, yielding a disproportionate contribution to the regional total. In contrast, permafrost-dominated northern and eastern regions show limited enhancement despite rapid warming: forests there are generally older, lower in stock volume, and more disturbance-prone (notably fire), corresponding to lower site quality. In addition, rising ecosystem emissions such as heterotrophic respiration under warmer conditions further offset carbon gains, keeping initial uptake low and constraining additional sink enhancement.

Together, these results establish a benchmark for Northern Eurasia, clarifying where and why estimates converge or diverge, and providing a basis for evaluating future climate–carbon feedback under continued anthropogenic forcing.

Conflict of Interest

The authors declare no conflicts of interest relevant to this study.

Availability Statement

Global CO_2 gridded flux fields from 14 atmospheric inversions in GCB2024 area available from the ICOS data portal (Luijkx et al., 2024). Data from the CMIP6 simulations are available from the ESGF archive (Cinquini et al., 2014). TRENDY v12 data were obtained from Sitch et al. (2024), FLUXCOM-RS data from the FluxCom ftp site (Jung et al., 2020), FLUXCOM-X data from the ICOS ERIC Carbon Portal (Nelson et al., 2024), CRU surface air temperature data from KNMI Climate Explorer (Harris et al., 2020), Global Fire Emissions Database (GFED) version 5 monthly trace gas and aerosol emissions data from Zenodo (van der Werf et al., 2025), and permafrost data extent from the CEDA Archive (Westermann et al., 2024a). Forest area data were obtained from the Oak Ridge National Laboratory DAAC (Hengeveld et al., 2015). The code and data for reproducing the main plots of the manuscript are publicly available and stored in the Zenodo archive (Melnikova et al., 2026).

Acknowledgments

We thank Dr Pavel Groisman of NOAA for encouraging this study. This work was supported by the Program for the Advanced Studies of Climate Change Projection (SENTAN, Grant JPMXD0722681344) from the Ministry of Education, Culture, Sports, Science and Technology of Japan; by KAKENHI (JP24K20979) of the Japan Society for the Promotion of Science; and by the European Union's Horizon Europe research and innovation program (EYE-CLIMA, Grant 101081395) (D.S.). We also thank all contributors to the flux data for the TRENDY-DGVM, FLUXCOM, and GCB2024 data sets.

References

Ciais, P., Yao, Y., Gasser, T., Baccini, A., Wang, Y., Lauerwald, R., et al. (2020). Empirical estimates of regional carbon budgets imply reduced global soil heterotrophic respiration. *National Science Review*, *8*(2), nwaa145. https://doi.org/10.1093/nsr/nwaa145

Cinquini, L., Crichton, D., Mattmann, C., Harney, J., Shipman, G., Wang, F., et al. (2014). The Earth System Grid Federation: An open infrastructure for access to distributed geospatial data. *Future Generation Computer Systems*, *36*, 400–417. https://doi.org/10.1016/j.future.2013.07.002

Deng, Z., Ciais, P., Tzompa-Sosa, Z. A., Saunois, M., Qiu, C., Tan, C., et al. (2022). Comparing national greenhouse gas budgets reported in UNFCCC inventories against atmospheric inversions. *Earth System Science Data*, *14*(4), 1639–1675. https://doi.org/10.5194/essd-14-1639-2022

Dolman, A. J., Shvidenko, A., Schepaschenko, D., Ciais, P., Tchebakova, N., Chen, T., et al. (2012). An estimate of the terrestrial carbon budget of Russia using inventory-based, eddy covariance and inversion methods. *Biogeosciences*, *9*(12), 5323–5340. https://doi.org/10.5194/bg-9-5323-2012

Eyring, V., Bony, S., Meehl, G. A., Senior, C. A., Stevens, B., Stouffer, R. J., & Taylor, K. E. (2016). Overview of the Coupled Model Intercomparison Project Phase 6 (CMIP6) experimental design and organization. *Geoscientific Model Development*, *9*(LLNL-JRNL-736881), 1937–1958. https://doi.org/10.5194/gmd-9-1937-2016

Fan, L., Wigneron, J.-P., Ciais, P., Chave, J., Brandt, M., Sitch, S., et al. (2023). Siberian carbon sink reduced by forest disturbances. *Nature Geoscience*, *16*(1), 56–62. https://doi.org/10.1038/s41561-022-01087-x

Filipchuk, A. N., Malysheva, N. V., Zolina, T. A., & Seleznev, A. A. (2023). Carbon stock in living biomass of Russian forests: New quantification based on data from the first cycle of the State Forest Inventory. *Central European Forestry Journal*, *69*(4), 248–261. https://doi.org/10.2478/forj-2023-0021

Friedlingstein, P., O'Sullivan, M., Jones, M. W., Andrew, R. M., Hauck, J., Landschützer, P., et al. (2025). Global Carbon Budget 2024. *Earth System Science Data*, *17*(3), 965–1039. https://doi.org/10.5194/essd-17-965-2025

Gasser, T., Crepin, L., Quilcaille, Y., Houghton, R. A., Ciais, P., & Obersteiner, M. (2020). Historical CO2 emissions from land use and land cover change and their uncertainty. *Biogeosciences*, *17*(15), 4075–4101. https://doi.org/10.5194/bg-17-4075-2020

Gier, B. K., Schlund, M., Friedlingstein, P., Jones, C. D., Jones, C., Zaehle, S., & Eyring, V. (2024). Representation of the terrestrial carbon cycle in CMIP6. *Biogeosciences*, *21*(22), 5321–5360. https://doi.org/10.5194/bg-21-5321-2024

Hansis, E., Davis, S. J., & Pongratz, J. (2015). Relevance of methodological choices for accounting of land use change carbon fluxes. *Global Biogeochemical Cycles*, *29*(8), 1230–1246. https://doi.org/10.1002/2014GB004997

Harris, I., Osborn, T. J., Jones, P., & Lister, D. (2020). Version 4 of the CRU TS monthly high-resolution gridded multivariate climate dataset. *Scientific Data*, *7*(1), 109. https://doi.org/10.1038/s41597-020-0453-3

Hengeveld, G. M., Gunia, K., Didion, M., Zudin, S., Clerkx, A. P. P. M., & Schelhaas, M. J. (2015). Global 1-degree maps of Forest area, carbon stocks, and biomass (pp. 1950–2010). https://doi.org/10.3334/ORNLDAAC/1296

Houghton, R. A., & Castanho, A. (2023). Annual emissions of carbon from land use, land-use change, and forestry from 1850 to 2020. *Earth System Science Data*, *15*(5), 2025–2054. https://doi.org/10.5194/essd-15-2025-2023

Huang, Y., Wang, Y.-P., & Ziehn, T. (2022). Nonlinear interactions of land carbon cycle feedbacks in Earth System Models. *Global Change Biology*, *28*(1), 296–306. https://doi.org/10.1111/gcb.15953

Isaev, A. S., Korovin, G. N., Bartalev, S. A., Ershov, D. V., Janetos, A., Kasischke, E. S., et al. (2002). Using remote sensing to assess Russian forest fire carbon emissions. *Climatic Change*, *55*(1), 235–249. https://doi.org/10.1023/A:1020221123884

Jin, Y., Keeling, R. F., Stephens, B. B., Long, M. C., Patra, P. K., Rödenbeck, C., et al. (2024). Improved atmospheric constraints on Southern Ocean CO_2 exchange. *Proceedings of the National Academy of Sciences*, *121*(6), e2309333121. https://doi.org/10.1073/pnas.2309333121

Jin, Y., Stephens, B. B., Long, M. C., Chandra, N., Chevallier, F., Hooghiem, J. J. D., et al. (2025). The Atmospheric Potential Oxygen forward Model Intercomparison Project (APO-MIP1): Evaluating simulated atmospheric transport of air-sea gas exchange tracers and APO flux products. *EGUsphere*, *2025*, 1–75. https://doi.org/10.5194/egusphere-2025-1736

Jung, M., Schwalm, C., Migliavacca, M., Walther, S., Camps-Valls, G., Koirala, S., et al. (2020). Scaling carbon fluxes from eddy covariance sites to globe: Synthesis and evaluation of the FLUXCOM approach. *Biogeosciences*, *17*(5), 1343–1365. https://doi.org/10.5194/bg-17-1343-2020

Kharuk, V. I., Ponomarev, E. I., Ivanova, G. A., Dvinskaya, M. L., Coogan, S. C. P., & Flannigan, M. D. (2021). Wildfires in the Siberian taiga. *Ambio*, *50*(11), 1953–1974. https://doi.org/10.1007/s13280-020-01490-x

Krankina, O. N., Sun, G., Shugart, H. H., Kharuk, V., Kasischke, E., Bergen, K. M., et al. (2004). Northern Eurasia. In G. Gutman, A. C. Janetos, C. O. Justice, E. F. Moran, J. F. Mustard, R. R. Rindfuss, et al. (Eds.), *Land change science: Observing, monitoring and understanding trajectories of change on the Earth's surface* (pp. 123–138). Springer Netherlands. https://doi.org/10.1007/978-1-4020-2562-4_8

Kukavskaya, E. A., Soja, A. J., Petkov, A. P., Ponomarev, E. I., Ivanova, G. A., & Conard, S. G. (2013). Fire emissions estimates in Siberia: Evaluation of uncertainties in area burned, land cover, and fuel consumption. *Canadian Journal of Forest Research*, *43*(5), 493–506. https://doi.org/10.1139/cjfr-2012-0367

Li, X., Ciais, P., Fensholt, R., Chave, J., Sitch, S., Canadell, J. G., et al. (2025). Large live biomass carbon losses from droughts in the northern temperate ecosystems during 2016-2022. *Nature Communications*, *16*(1), 4980. https://doi.org/10.1038/s41467-025-59999-2

Liu, L., Zhuang, Q., Zhao, D., Wei, J., & Zheng, D. (2024). The fate of deep permafrost carbon in northern high latitudes in the 21st century: A process-based modeling analysis. *Earth's Future*, *12*(11), e2024EF004996. https://doi.org/10.1029/2024EF004996

Luijkx, I., Peters, W., Lloret, Z., Zhao, M., Niwa, Y., Jacobson, A. R., et al. (2024). Global CO2 gridded flux fields from 14 atmospheric inversions in GCB2024 [Dataset]. *ICOS ERIC—Carbon Portal*. https://doi.org/10.18160/4R5W-VNBV

McDowell, N. G., Allen, C. D., Anderson-Teixeira, K., Aukema, B. H., Bond-Lamberty, B., Chini, L., et al. (2020). Pervasive shifts in forest dynamics in a changing world. *Science*, *368*(6494), eaaz9463. https://doi.org/10.1126/science.aaz9463

McKay, D. I. A., Sakschewski, B., Roman-Cuesta, R. M., Dakos, V., Flores, B. M., Hessen, D. O., et al. (2023). Section 1. Earth system tipping points. Chapter 1.3 tipping points in the biosphere. In *The global tipping points report 2023*. University of Exeter.

Melnikova, I., Yokohata, T., Schepaschenko, D., Sitch, S., & Maksyutov, S. (2026). Land carbon sink distribution in Northern Eurasia is driven by climate change (data and code) [Dataset]. *Zenodo*. https://doi.org/10.5281/zenodo.19188105

Miyahara, M., Takenaka, C., Tomioka, R., & Ohta, T. (2011). Root responses of Siberian larch to different soil water conditions. *Hydrological Research Letters*, *5*, 93–97. https://doi.org/10.3178/hrl.5.93

Nelson, J. A., Walther, S., Gans, F., Kraft, B., Weber, U., Novick, K., et al. (2024). X-BASE: The first terrestrial carbon and water flux products from an extended data-driven scaling framework, FLUXCOM-X. *Biogeosciences*, *21*(22), 5079–5115. https://doi.org/10.5194/bg-21-5079-2024

Norby, R. J., Loader, N. J., Mayoral, C., Ullah, S., Curioni, G., Smith, A. R., et al. (2024). Enhanced woody biomass production in a mature temperate forest under elevated CO_2. *Nature Climate Change*, *14*(9), 983–988. https://doi.org/10.1038/s41558-024-02090-3

O'Sullivan, M., Sitch, S., Friedlingstein, P., Luijkx, I. T., Peters, W., Rosan, T. M., et al. (2024). The key role of forest disturbance in reconciling estimates of the northern carbon sink. *Communications Earth & Environment*, *5*(1), 705. https://doi.org/10.1038/s43247-024-01827-4

Ponomarev, E. I., Zabrodin, A. N., Shvetsov, E. G., & Ponomareva, T. V. (2023). Wildfire intensity and fire emissions in Siberia. *Fire*, *6*(7), 246. https://doi.org/10.3390/fire6070246

Qin, Z., Zhu, Y., Canadell, J. G., Chen, M., Li, T., Mishra, U., & Yuan, W. (2024). Global spatially explicit carbon emissions from land-use change over the past six decades (1961–2020). *One Earth*, *7*(5), 835–847. https://doi.org/10.1016/j.oneear.2024.04.002

Remaud, M., Ma, J., Krol, M., Abadie, C., Cartwright, M. P., Patra, P., et al. (2023). Intercomparison of Atmospheric Carbonyl Sulfide (TransCom-COS; part one): Evaluating the impact of transport and emissions on tropospheric variability using ground-based and aircraft data. *Journal of Geophysical Research: Atmospheres*, *128*(6), e2022JD037817. https://doi.org/10.1029/2022JD037817

Romanov, A. A., Tamarovskaya, A. N., Gloor, E., Brienen, R., Gusev, B. A., Leonenko, E. V., et al. (2022). Reassessment of carbon emissions from fires and a new estimate of net carbon uptake in Russian forests in 2001–2021. *Science of the Total Environment*, *846*, 157322. https://doi.org/10.1016/j.scitotenv.2022.157322

Romanovskaya, A., Korotkov, V. N., Polumieva, P. D., Trunov, A. A., Vertyankina, V. Y., & Karaban, R. T. (2020). Greenhouse gas fluxes and mitigation potential for managed lands in the Russian Federation. *Mitigation and Adaptation Strategies for Global Change*, *25*(4), 661–687. https://doi.org/10.1007/s11027-019-09885-2

Romanovskaya, A., Nahutin, A., Ginzburg, V., Grbar, V., Imshennik, E., Karaban, R., & Korotkov, V. (2022). *National inventory report on anthropogenic emissions by sources and removals by Sinks of greenhouse gases not controlled by the Montreal protocol for 1990–2020 (in Russian)*. Yu. A. Izrael Institute of Global Climate and Ecology (IGCE). Retrieved from https://elibrary.ru/item.asp?id=53434805

Romanovskaya, A., Nahutin, A., Ginzburg, V., Grbar, V., Zelenova, M. S., Imshennik, E., et al. (2025). *National inventory report on anthropogenic greenhouse gas emissions from sources and their removals by Sinks for 1990–2023 (in Russian)*. Yu. A. Izrael Institute of Global Climate and Ecology (IGCE). Retrieved from https://unfccc.int/sites/default/files/resource/RUS_NIR_2025_v1_rev_2025-04-18.pdf

Schepaschenko, D., Moltchanova, E., Fedorov, S., Karminov, V., Ontikov, P., Santoro, M., et al. (2021). Russian forest sequesters substantially more carbon than previously reported. *Scientific Reports*, *11*(1), 12825. https://doi.org/10.1038/s41598-021-92152-9

Schepaschenko, D., Moltchanova, E., Shvidenko, A., Blyshchyk, V., Dmitriev, E., Martynenko, O., et al. (2018). Improved estimates of biomass expansion factors for Russian forests. *Forests*, *9*(6), 312. https://doi.org/10.3390/f9060312

Schepaschenko, D., Shvidenko, A. Z., Lesiv, M. Y., Ontikov, P. V., Shchepashchenko, M. V., & Kraxner, F. (2015). Estimation of forest area and its dynamics in Russia based on synthesis of remote sensing products. *Contemporary Problems of Ecology*, *8*(7), 811–817. https://doi.org/10.1134/S1995425515070136

Schuur, E. A. G., Abbott, B. W., Commane, R., Ernakovich, J., Euskirchen, E., Hugelius, G., et al. (2022). Permafrost and climate change: Carbon cycle feedbacks from the warming Arctic. *Annual Review of Environment and Resources*, *47*(1), 343–371. https://doi.org/10.1146/annurev-environ-012220-011847

Shvidenko, A., Ciais, P., Patra, P. K., Bastos, A., Maksyutov, S., Lauerwald, R., et al. (2025). A system reanalysis of the current greenhouse gases budget of terrestrial ecosystems in Russia. *Global Biogeochemical Cycles*, *39*(10), e2025GB008540. https://doi.org/10.1029/2025GB008540

Shvidenko, A. Z., & Schepaschenko, D. G. (2013). Climate change and wildfires in Russia. *Contemporary Problems of Ecology*, *6*(7), 683–692. https://doi.org/10.1134/S199542551307010X

Sitch, S., O'Sullivan, M., Robertson, E., Friedlingstein, P., Albergel, C., Anthoni, P., et al. (2024). Trends and drivers of terrestrial sources and sinks of carbon dioxide: An overview of the TRENDY project. *Global Biogeochemical Cycles*, *38*(7), e2024GB008102. https://doi.org/10.1029/2024GB008102

Terrer, C., Jackson, R. B., Prentice, I. C., Keenan, T. F., Kaiser, C., Vicca, S., et al. (2019). Nitrogen and phosphorus constrain the CO_2 fertilization of global plant biomass. *Nature Climate Change*, *9*(9), 684–689. https://doi.org/10.1038/s41558-019-0545-2

Tokarska, K. B., Stolpe, M. B., Sippel, S., Fischer, E. M., Smith, C. J., Lehner, F., & Knutti, R. (2020). Past warming trend constrains future warming in CMIP6 models. *Science Advances*, *6*(12), eaaz9549. https://doi.org/10.1126/sciadv.aaz9549

Tramontana, G., Jung, M., Schwalm, C. R., Ichii, K., Camps-Valls, G., Ráduly, B., et al. (2016). Predicting carbon dioxide and energy fluxes across global FLUXNET sites with regression algorithms. *Biogeosciences*, *13*(14), 4291–4313. https://doi.org/10.5194/bg-13-4291-2016

Upton, S., Reichstein, M., Gans, F., Peters, W., Kraft, B., & Bastos, A. (2024). Constraining biospheric carbon dioxide fluxes by combined top-down and bottom-up approaches. *Atmospheric Chemistry and Physics*, *24*(4), 2555–2582. https://doi.org/10.5194/acp-24-2555-2024

van der Werf, G., Randerson, J., van Wees, D., Chen, Y., Giglio, L., Hall, J., et al. (2025). Global Fire Emissions Database version 5 (GFED5) [Dataset]. *Zenodo*. https://doi.org/10.5281/zenodo.16794692

Walker, A. P., De Kauwe, M. G., Medlyn, B. E., Zaehle, S., Iversen, C. M., Asao, S., et al. (2019). Decadal biomass increment in early secondary succession woody ecosystems is increased by CO2 enrichment. *Nature Communications*, *10*(1), 454. https://doi.org/10.1038/s41467-019-08348-1

Wendland, K. J., Lewis, D. J., & Alix-Garcia, J. (2014). The effect of decentralized governance on timber extraction in European Russia. *Environmental and Resource Economics*, *57*(1), 19–40. https://doi.org/10.1007/s10640-013-9657-8

Westermann, S., Barboux, C., Bartsch, A., Delaloye, R., Grosse, G., Heim, B., et al. (2024a). *ESA permafrost climate change initiative (Permafrost_cci): Permafrost extent for the Northern Hemisphere, v4.0 [Application/xml]*. NERC EDS Centre for Environmental Data Analysis. https://doi.org/10.5285/93444BC1C4364A59869E004BF9BFD94A

Westermann, S., Barboux, C., Bartsch, A., Delaloye, R., Grosse, G., Heim, B., et al. (2024b). *ESA Permafrost Climate Change Initiative (Permafrost_CCI): Permafrost version 4 data products*. NERC EDS Centre for Environmental Data Analysis.

Zheng, B., Ciais, P., Chevallier, F., Chuvieco, E., Chen, Y., & Yang, H. (2021). Increasing forest fire emissions despite the decline in global burned area. *Science Advances*, *7*(39), eabh2646. https://doi.org/10.1126/sciadv.abh2646